Resilience to Chronic Stress Is Associated with Specific Neurobiological, Neuroendocrine and Immune Responses.

Author list:

Anand Gururajan[1,2$], Marcel van de Wouw[1,2], Marcus Boehme[1,2], Thorsten Becker[1,2], Rory O'Connor[1,2], Thomaz F S Bastiaanssen[1,2], Gerard M Moloney[1], Joshua M Lyte[2], Ana Paula Ventura Silva[2], Barbara Merckx[1], Timothy G Dinan[2,4], John F Cryan[1,2]

[1]Department of Anatomy & Neuroscience, University College Cork, Ireland

[2]APC Microbiome Ireland, University College Cork, Ireland,

[4]Department of Psychiatry & Neurobehavioural Science, University College Cork, Ireland.

[$]Current address: Brain & Mind Centre, University of Sydney, New South Wales, Australia

Corresponding authors: John F Cryan (Email:j.cryan@ucc.ie) and Anand Gururajan (anand.gururajan@sydney.edu.au)

Abstract

Research into the molecular basis of stress resilience is a novel strategy to identify potential therapeutic strategies to treat stress-induced psychopathologies such as anxiety and depression. Stress resilience is a phenomenon which is not solely driven by effects within the central nervous system (CNS) but involves multiple systems, central and peripheral, which interact with and influence each other. Accordingly, we used the chronic social defeat stress paradigm and investigated specific CNS, endocrine and immune responses to identify signatures of stress-resilience and stress susceptibility in mice. Our results showed that mice behaviourally susceptible to stress (indexed by a reduction in social interaction behaviour) had higher plasma corticosterone levels and adrenal hypertrophy. An increase in inflammatory circulating monocytes was another hallmark of stress susceptibility. Furthermore, prefrontal cortex mRNA expression of corticotrophin-releasing factor (*Crf*) was increased in susceptible mice relative to resilient mice. We also report differences in hippocampal synaptic plasticity between resilient and susceptible mice. Ongoing studies will interpret the functional relevance of these signatures which could potentially inform the development of novel psychotherapeutic strategies.

Keywords stress resilience; neuroendocrine; corticotrophin-releasing factor; prefrontal cortex; synaptic plasticity; inflammatory monocytes

1. Introduction

Stress-induced psychopathologies such as anxiety and major depression are the most prevalent mental health disorders worldwide and impose a significant burden on society (WHO, 2017). A conventional approach to develop therapeutic strategies in this context is to create animal models which incorporate chronic stress exposure (Slattery and Cryan, 2017). Such paradigms enable the identification of causative links between stress, its effects on the central nervous system and the onset of behaviours which are clinically relevant. These links, in turn, form the basis for developing pharmacotherapeutics. However, over the last two to three decades our perspective of stress as a risk factor with a predetermined detrimental outcome has shifted significantly to one where stress induces a spectrum of phenotypes and at opposing ends lie individuals who are stress-resilient and stress-susceptible (Franklin et al., 2012; Pfau and Russo, 2015). From a therapeutic standpoint, identifying the central and peripheral processes which underlie the former could form the basis for novel therapeutic strategies which not only treat stress-induced psychopathologies but also build resilience against future stress exposure (Kentner et al., 2018).

The chronic social defeat stress paradigm is a popular preclinical methodology that has been used in the study of stress-resilience and susceptibility (Pryce and Fuchs, 2017). Classification is typically based on a test of social behaviour following the stress paradigm; mice which display increased social avoidance are labelled as susceptible and conversely, mice with intact social behaviour are considered resilient. Some of the recent findings which have emerged from studies using this experimental approach include the identification of differentially expressed genes between susceptible and resilient mice linked to CNS myelination (Laine et al., 2018) and DNA methylation in the bed nucleus of the stria terminalis and hippocampus

(Hammels et al., 2015) as well as contrasting peripheral and central immune signatures (Ambrée et al., 2018). Susceptible mice have also been shown to diverge from resilient mice in terms of the activity of the hypothalamic-pituitary-adrenal (HPA) axis (Jochems et al., 2015) which is known to be dysfunctional in stress-induced psychopathologies such as anxiety and major depression (Zorn et al., 2017).

However, to our knowledge, no study has yet combined behavioural readouts with systemic immune readouts, hippocampal electrophysiological recordings and gene expression data from relevant brain regions as functional readouts of the stress response. Such an integrated, systems-based approach would provide a more in-depth understanding of the impact of chronic stress on the mouse as a whole. To this end, the goal of our study was to use several orthogonal techniques to systematically identify putative central and peripheral signatures of stress-resilience and stress-susceptibility in mice exposed to a modified version of the chronic social defeat stress paradigm.

2. Materials & Methods

2.1 Animals & Housing

Adult male mice were used for this study. Breeding pairs (B6;129-*Gt(ROSA)26Sor*$^{tm1(CAG-cas9,-EGFP)Fezh}$/J) were purchased from The Jackson Laboratory (https://www.jax.org/strain/024857) to establish an in-house breeding colony for planned follow-up CRISPR-cas9 experiments. Approximately one week before commencement of social defeat sessions, all mice were singly housed and weighed daily over the course of the experimental protocol (Figure 1). Percentage change in weight gain was calculated based on body weights recorded the day before the first defeat (day 0) and the day after the last defeat (day 11). For the chronic social defeat stress procedure, non-experimental singly housed adult male CD1 were used as aggressors (Envigo, UK). Mice were kept under a 12 hr light/dark cycle (ON 7:30AM, OFF 7:30PM) in a temperature/humidity controlled environment (21℃, 55.5%) with food and water *ad libitum*.

(Insert Figure 1 here)

2.2 Chronic social defeat stress

Mice were randomly assigned to either the social defeat stress (n=32) or control groups (n=27). Chronic social defeat stress was carried out daily for 10 consecutive days (see Fig 1 for experimental timeline) by the same researcher as previously described but with slight modifications (Savignac et al., 2011). Prior to the defeat sessions, all CD1 aggressor mice were tested for aggressiveness over two separate days. A CD1 mouse was directly exposed to another CD1 mouse until the first attack. Mice with the shortest attack latencies were selected as aggressors to be used in subsequent social defeats. For each defeat session, test mice were subjected to a different aggressor CD1 mouse each day over the 10 days. The session would involve a single initial exposure of the test mouse to the aggressive CD1 in a

clean cage with fresh bedding (to eliminate effects of coprophagy) until the first attack, expression of submissive posturing or until 5 mins had passed. The latency to attack or display a submissive posture was recorded. The mice were then separated by a perforated Plexiglas® wall that allowed only non-physical contact for 2 hrs. Subsequently, the separator was removed and, after another defeat, mice were transferred back to their home-cage. All defeat sessions were carried out in the mornings during the light cycle. Control mice remained in their home-cages over the course of the stress protocol but were handled to an equal extent as the stressed mice in the process of measuring daily body weight and collecting tail-blood samples. Following social defeat, the number of mice used for each experimental procedure is tabulated below.

(Insert Table 1 here)

2.3 Social interaction test

All mice were habituated to the test room for 1 hr prior to testing which was carried out during the light cycle and under-red light (5 lux) to reduce interference of potential anxiogenic factors with social interaction behaviour. In the first 2.5 min trial (Trial 1), the test mouse was placed into a plastic box (41 × 32 × 24 cm) containing a wire mesh cage (9.5 × 7.5 × 7.0 cm) against one wall and allowed to explore freely. The mouse was then returned to its home cage for 1 min. During this time, an unfamiliar aggressor CD1 mouse was placed inside the wire mesh cage. This was followed by a second 2.5 min trial (Trial 2) in which the test mouse was allowed to explore the area freely in the presence of the caged CD1. At the end of the social interaction test, mice were returned to their respective home cages and the arena and mesh were cleaned with 70% ethanol. Trials were video-recorded and analysed using EthoVision 3.1 (Noldus, Wageningen, Netherlands) to quantify locomotor activity and time spent in an interaction zone (IZ) 8cm around the wire mesh cage (Supplementary Figure 1).

The experimenter was blind to group assignment during video analysis. The time spent in the IZ during the first and the second trials were used to calculate the social interaction ratio (time spent in IZ during Trial 2/time spent in IZ during Trial 1). Mice with ratios above 1 were classified as resilient and those with ratios less than 1 were classified as susceptible.

2.4 Plasma collection & Corticosterone assay

Tail bleeds were carried out within 1 hour of the lights turning on (0730-0830). The tail of an unrestrained mouse was held between two fingers and a diagonal incision was made on the tip (2mm) using a new single-edge razor blade. As previously described, the tail was gently squeezed by the two fingers of the researcher until 20-30µl of blood was collected using Lithium-Heparin coated capillary tubes (Sigma-Aldrich, St Louis, Missouri, United States) which was subsequently deposited into an eppendorf containing EDTA and centrifuged at 3500g at 4°C for 15 min (Burokas et al., 2017). Plasma was aspirated and stored at -20°C. Samples were collected on the day before the first defeat (day 0) and on the day after the last defeat (day 11). Plasma samples were analysed in duplicate using the Enzo® Corticosterone ELISA kit plate (Enzo® , Exeter, United Kingdom) according to the manufacturer's instructions. The lowest detection threshold was 27pg/ml and concentrations expressed are in ng/ml. ELISA plates were read using a Multiskan® microplate photometer (Thermofisher Scientific® , Waltham, MA, USA) at 405nm. Across the 10 plates we used, the inter-assay coefficient of variation was 10% and the average intra-assay coefficient of variation was 2.4%. These values fall within the manufacturer's guidelines.

2.5 Tissue collection

Mice were sacrificed by cervical decapitation. The brain was excised and four brain regions with critical roles in the stress response were dissected using a brain slicer – prefrontal cortex (PFC: A/P 2.2 to 1.70, M/L ± 0.8, DV -1 to -3.2), bed nucleus of the stria terminalis (BNST: A/P 0.26 to -0.1, M/L ± 0 to ± 1.0, DV -4.0 to -4.8), amygdala (AMG: A/P -1.06 to -2.06, M/L ± 2.2 to ± 3.2, DV -3.9 to -5.2) and hippocampus (HIP: A/P -2.30 to -3.40, M/L ± 1 to ± 3.4, DV -1.2 to -5). Tissue was snap-frozen on dry ice before being stored at -80°C until further analysis.

2.6 Gene expression analysis - Quantitative real-time polymerase chain reaction (qRT-PCR)

Total RNA was extracted using the miRVana™ miRNA Isolation kit (Ambion/Life Technologies, Paisley, UK) according to the manufacturer's instructions. RNA concentrations were quantified using a NanoDrop™ spectrophotometer (Thermofisher Scientific®, Waltham, MA, USA) and only samples with 260/280 ratios of greater than 1.8 were used. RNA was reverse-transcribed to complementary DNA using the Applied Biosystem® High Capacity cDNA Reverse Transcription Kit (10X RT Buffer, 25X dNTP mix (100mM), 10X RT Random Primers, Multiscribe® Reverse Transcriptase) on the Applied Biosystem® GeneAmp PCR System 9700 (Thermofisher®, Waltham, MA, USA). qRT-PCR was carried out on the StepOnePlus® PCR machine (Thermofisher®, Waltham, MA, USA) using the following primer assays (Table 2) designed by Integrated DNA Techologies (Skokie, Illinois, USA).

(Insert Table 2 here)

Samples were heated to 95°C x 10 min, and then subjected to 40 cycles of amplification by melting at 95°C x 15 s and annealing at 60°C x 1 min. Experimental samples were run in duplicates with 1.33 µL complementary DNA (cDNA) per reaction. To check for amplicon contamination, each run also contained template free controls for each probe used. PCR data

were normalized using *β-actin* and transformed using the $\Delta\Delta C_t$ method as previously described (Stilling et al., 2018).

2.7 Electrophysiology

Acute brain slice preparation. Mice were anesthetized with isoflurane (Abbot, Chicago, USA). Anesthesia was maintained until mice were decapitated. Once the pain reflexes were absent, mice were transcardially perfused using chilled 20 ml NMDG-aCSF (in mM: N-methyl-d-glucamine 92.0, KCl 2.5, NaH_2PO_4-H_2O 1.25, $NaHCO_3$ 30.0, HEPES 20.0, Thiourea 2.0, Ascorbate 5.0, Na-Pyruvate 3.0, Glucose 25.0, $CaCl_2$ 0.5, $MgSO_4$ 10.0). Immediately after the animal was exsanguinated, it was decapitated and its brain carefully removed. The removed brain was immediately mounted onto a vibratome (VT1000S, Leica Biosystems, Nussloch, Germany) and brain slices (transverse, 300µm thick) that contained the hippocampus were kept. The obtained slices were kept in NMDG-aCSF for 12 min at 32 - 34°C. Subsequently, they were kept at room temperature in Holding-aCSF (in mM: NaCl 92.0, KCl 2.5, NaH2PO4-H2O 1.25, NaHCO3 30.0, HEPES 20.0, Thiourea 2.0, Ascorbate 5.0, Na-Pyruvate 3.0, Glucose 25.0, $CaCl_2$ 2.0, $MgSO_4$ 2.0) for 1h before the beginning of the recordings. Throughout the slicing process, from slicing to holding, brain slices were oxygenated with Carboxygen (5% O_2/95% CO_2; Irish Gas).

Recordings. Recordings were obtained in a multi-electrode array chip with a 5x13 electrode layout (MEA60-5x13, Qwane Biosciences, Lausanne, Switzerland) connected to a MEA2100 Headstage (Multichannel Systems, Reutlingen, Germany) connected to a digitizer (Interface Board 3.0 Multiboot, Multichannel Systems, Reutlingen, Germany) and controlled through MCRack software (Version 4.6.2, Multichannel Systems, Reutlingen, Germany). Sampling rate

was 20kHz. Once a brain slice was placed in the MEA-chip, it was kept in place with a slice anchor, while oxygenated aCSF (in mM: NaCl 119.0, KCl 2.5, NaH_2PO_4-H_2O 1.25, $NaHCO_3$ 24.0, Glucose 12.5, $CaCl_2$ 2.0, $MgSO_4$ 2.0) was provided at a flow rate of about 4 mL/min using a peristaltic pump (PPS2, Multichannel Systems, Reutlingen, Germany). The temperature in the MEA-chip was maintained at 37°C (PH01, Multichannel Systems, Reutlingen, Germany). Electrodes located in the stratum radiatum and/or stratum lacunosum-moleculare of the CA1 region were used to stimulate Schaffer collaterals. Once administration of a 75µA bipolar square pulse resulted in a field excitatory postsynaptic potential (fEPSP) in the stratum radiatum of CA1, the same pulse was delivered every 30s until the peak amplitude of the fEPSP (measured from baseline) remained stable. Subsequently, an input-output (I/O) curve was recorded by applying current steps through the same stimulation electrode (2, 5, 10, 25, 50, 100, 150, and 200 µA). Based on this I/O curve, the stimulation intensities that resulted in an fEPSP with a peak amplitude of 30% of max amplitude (30% stimulus intensity) and an fEPSP with a peak amplitude of 50% of max amplitude (50% stimulus intensity) were chosen for paired pulse recordings with four different interpulse intervals (IPI; 25, 50, 100, 200 ms). For each IPI 10 paired pulses were recorded at each stimulus intensity and the average of these 10 pairs was used for analysis. Overall, the parameter used for analysis was fEPSP slope (calculated between 30 and 50% of the peak amplitude). The paired-pulse ratio (PPR) was computed as PPR = $f\text{EPSPslope}_{Pulse2}/f\text{EPSPslope}_{Pulse1}$. If PPR > 1 we speak of paired-pulse facilitation (PPF) and if it is PPR <1 we speak of paired-pulse depression (PPD).

2.8 Flow cytometry

Trunk blood (60µL) was collected in EDTA coated tubes and processed on the same day for flow cytometry. Blood was resuspended in 10 mL home-made red blood cell lysis buffer (15.5

mM NH_4Cl, 1.2 mM $NaHCO_3$, 0.01 mM tetrasodium EDTA diluted in deionised water) for 4 min. Blood samples were subsequently centrifuged (1500g, 5 min) and resuspended in 45µL staining buffer (autoMACS Rinsing Solution (Miltenyi, 130-091-222) supplemented with MACS BSA stock solution (Miltenyi, 130-091-376)). For the staining procedure, 5 µL of FcR blocking reagent (Miltenyi, 130-092-575) was added to each sample. Samples were subsequently incubated with a mix of antibodies (5 µL CD11b-FITC (Miltenyi, 130-081-201), 2 µL LY6C-PerCP-Vio700 (Miltenyi, 130-111-782) and 5 µL MHC-II-APC (Miltenyi, 130-102-139) and incubated for 30 min on ice. Samples were subsequently fixed using 4% paraformaldehyde for 30 min on ice and finally resuspended in staining buffer. The following day, samples were analysed on the BD FACS Calibur flow cytometry machine. Data were analysed using FlowJo (version 10). PBMCs were gated based on their FSC-SSC, after which granulocytes (CD11b+, SSC(high)) and CD11b+, SSC(low) cells were selected. The latter population was subsequently used to identify inflammatory monocytes (CD11b+, SSC(low), LY6C(high)) and CD11b+, SSC(low), LY6C(low) cells, which consist mainly of resident monocytes (Ginhoux and Jung, 2014; Lessard et al., 2017). The investigated cell populations were normalised to PBMC levels. CD11b expression on target populations was quantified by median fluorescent intensity (MFI), whereas MHC-II expression was investigated by quantification of MHC-II+ cells, as expression of the MHC-II receptor was not prevalent on all cells.

2.9 Statistical Analysis

Statistical analysis was done in an R software environment. All data were assessed for normality using the Shapiro-Wilk test and Levene's test for equality of variance. Outliers were removed from each group using the ROUT method (Motulsky and Brown, 2006). Normally distributed data were analysed using a one-way ANOVA followed by Bonferroni-corrected

two-tailed t-tests for planned between group comparisons (control vs susceptible, control vs resilient, resilient vs susceptible) (Laine et al., 2018). Repeated measures ANOVA was used for analysis of electrophysiological input/output recordings with stress phenotype as between-subjects factor and stimulation as within-subjects factor. Paired-pulse recordings at different IPIs were analysed using one-way ANOVA with stress phenotype as factor. Differences were further examined using Bonferroni-corrected two-tailed t-tests for between group comparisons. For datasets in which the condition of normality was violated the Kruskal-Wallis test was used followed by Dunn-Bonferroni corrected tests for planned between group comparisons as above. Permutational multivariate analysis of variance (PERMANOVA) was used to identify relationships of significance between variables. A p-value of <0.05 was deemed significant in all cases.

3. Results

3.1 Chronic social defeat stress

In carrying out our social defeat stress paradigm, we made two key observations which we report here. Firstly, over the course of the 10 days, we noted that on average mice were socially defeated by an aggressive CD1 mice at least 60% of the time. Secondly, on days when there was aggression, the average latency to attack the test mouse during the first exposure was 100 sec (Supplementary Figure 2). None of our experimental mice suffered from any wounds.

The chronic social defeat stress paradigm had a significant effect on social behaviour ($\chi^2(2)=22.13$, $p<0.001$). Subsequent classification based on social interaction ratios revealed a lower proportion of susceptible mice (14/32) compared to resilient mice (18/32). Between-group comparisons revealed social behaviour of susceptible mice was significantly impaired compared to resilient mice ($p<0.001$) and control mice ($p<0.01$). There was also a significant increase in social behaviour in resilient mice compared to controls ($p<0.05$) (Fig 2a). There was no difference in the percentage days of aggression or in the latency to attack or display submissive posture between resilient and susceptible mice (Supplementary Figure 2).

3.2 Locomotor Activity

During Trial 1 of the social interaction test when there was no CD1 in the mesh cage, there were between-group differences in locomotor activity ($\chi^2(2)=8.17$, $p<0.05$) with a significant reduction in locomotor activity of resilient mice compared to controls ($p<0.05$). In Trial 2, the presence of a CD1 mouse decreased locomotor activity in all mice compared to Trial 1

(control: $p<0.001$; susceptible $p<0.01$; resilient: $p<0.01$) but there were no between-group differences (Fig 2b).

3.3 Plasma Corticosterone (CORT)

At baseline (Day 0) there were no statistically significant differences between groups in plasma CORT. However, differential effects emerged on the day after the last defeat session (Day 11) ($F_{(2,50)=}12.31$, $p<0.001$). In particular, plasma CORT was significantly elevated in susceptible mice compared to controls ($p<0.001$) and resilient mice ($p<0.01$) (Fig 2c). Examining the relationship between social behaviour and plasma CORT, PERMANOVA of all three groups followed by pairwise PERMANOVA revealed that the centroid for susceptible mice is distinct from controls ($F_{(1,39)}=21.6$, $p<0.001$) and resilient mice ($F_{(1,27)}=9.76$, $p<0.001$) but not different between resilient and controls (Fig 2d).

3.4 Body & Organ Weights

There was an overall effect of stress on body weight gain ($F_{(2,56)}=8.54$, $p<0.001$). Between-group comparisons revealed a significant decrease in weight in resilient mice ($p<0.01$) and a trend towards a reduction in susceptible mice ($p=0.079$) compared to controls (Fig 2e). Stress differentially affected the weight of adrenal glands ($F_{(2,37)}=16.11$, $p<0.001$) with increases in susceptible ($p<0.05$) and resilient mice ($p<0.05$) compared to controls; adrenal weight was also significantly greater in susceptible mice compared to resilient mice ($p<0.05$) (Fig 2f). There was a trend towards an effect of stress on thymus weight ($F_{(2,40)}=2.65$, $p=0.08$) and between-group comparisons revealed a significant reduction in resilient mice ($p<0.05$) compared to control mice (Fig 2g). Stress had a potentiating effect on spleen weight in all mice ($F_{(2,41)}=6.784$, $p<0.01$). Between group-comparisons revealed an increase in susceptible

(p<0.01) and trend towards an increase in resilient mice (p=0.086) relative to controls (Fig 2h).

(Insert Figure 2 here)

3.5 Gene Expression in the Brain

Chronic social defeat stress affected expression of PFC *Crf* mRNA ($\chi^2(2)=10.554$, p<0.01) (Fig 3a). In particular, between-group comparisons revealed a significant difference in expression between susceptible mice and resilient mice (p<0.01). There were no significant effects of chronic stress on gene expression in the AMG (Fig 3b). Chronic stress upregulated mRNA expression of HIP *Crfr1* ($F_{(2,38)}=3.685$, p<0.05) with significance increase in resilient mice compared to control mice (p<0.05) (Fig 3c). There were no significant effects of chronic stress on gene expression in the BNST (Fig 3d).

(Insert Figure 3 here)

3.6 Hippocampal electrophysiology

Generally, our I/O curves did not reach a maximum, therefore the lower stimulus intensity cannot be considered to be 30% of the maximum slope but rather <30% and this also is the case for the higher stimulation intensity used. The I/O curves of fEPSPs at the SC-CA1 synapse of resilient mice suggests a tendency towards elevated excitability compared to those of control and stress-susceptible mice (Fig 4a). An easily excitable synapse displays elevated neurotransmitter release probability or paired-pulse facilitation (PPF) with a PPR of around 1.

At both stimulation strengths and at all IPIs we observed PPF, meaning a PPR >1 at the SC-CA1 synapse in acute hippocampal slices. This observation was not unexpected, as the SC-CA1 synapse is considered to have low vesicle release probability (Hasegawa et al., 2018; Hinds et al., 2003; Wu and Saggau, 1994). However, Petersen et al., (2013) have shown that

lateral perforant pathway inputs onto granule cells in the dentate gyrus express PPF or PPD depending on stimulation intensity and interpulse intervals. Thus, we were interested if the use of different stimulation strengths and IPIs would unveil phenotype-dependent differences in synaptic physiology.

When stimulated with lower intensity (<30%, Fig 4b), PPF differed between groups at IPIs of both 25ms ($F_{(2,30)}$=3.106, p=0.059) and 50ms ($\chi^2(2)$=6.372, p<0.05). At an IPI of 25ms, both stress susceptible and stress resilient mice displayed lowered PPF which did not reach significance (p=0.088 and p=0.174, respectively). At an IPI of 50 ms, PPF was reduced in resilient mice (p=0.054) but not significantly in susceptible mice (p=0.165) compared to control mice. No differences were observed at higher IPIs.

When challenged with higher stimulation current (<50%, Fig 4c), at an IPI of 100ms, PPF also differed between groups ($\chi^2(2)$=7.172, p<0.05); in particular, the PPF of resilient mice trended towards being reduced compared to controls (p=0.065) and susceptible mice, although not significantly (p=0.109). Furthermore at an IPI of 200ms there was a trend towards an effect on PPR ($\chi^2(2)$=5.05, p=0.08) with PPR of resilient mice tending towards 1 and reduced comparable to both the PPR of control (p=0.153) and susceptible mice (p=0.252).

(Insert Figure 4 here)

3.7 Flow cytometry

Stress increased the proportion of inflammatory monocytes (CD11b+, SSC(low), Ly-6C(high) cells) ($F_{(2,34)}$=5.68, p<0.01) in all mice. Between group comparisons revealed a significant increase in susceptible mice (p<0.05) and a trend towards significance in resilient mice (p=0.07) compared to controls (Fig 5d). However, the proportion of CD11b+, SSC(low), Ly-

6C(low) cells, consisting of mainly resident monocytes, remained unchanged (Fig 5e). There were no between-group differences in the proportion of MHC-II+ (Fig 5f) or CD11b expressing inflammatory monocytes (Fig 5g). Stress increased the proportion of circulating granulocytes ($F_{(2,35)}$=4.29, $p<0.05$) with between-group comparisons revealing a significant increase in resilient mice compared to controls ($p<0.05$) (Fig 5h). The percentage of MHC-II+ granulocytes and CD11b receptor expression were not different between groups (Fig 5i, j).

(Insert Figure 5 here)

4. Discussion

The response to stress involves multiple systems and understanding the biological constructs that are responsive to resilience may pave the way for novel therapeutic strategies for stress-related disorders. Here we show what is to our knowledge the first study to explore the impact of chronic social defeat stress on physiology, neuroendocrine systems, CNS gene expression, hippocampal synaptic plasticity and peripheral innate immune responses with a view to identifying signatures of stress resilience and susceptibility.

For our investigation, we used a modified version of the chronic social defeat stress paradigm which is now wideley used in the field (Pryce and Fuchs, 2017). However, important variables which could influence individual differences in stress response include the latency to attack or adopt a defensive posture and also the days of aggression. One study reported that the latency to attack was approximately 14 sec in male C57BL/6J with Swiss mice as aggressors over a 5-day defeat protocol (Henriques-Alves and Queiroz, 2016). Another which used female C57BL/6J reported the latency to attack and the days of aggressive behaviour as a percentage were approximately 125 sec and 60%, respectively, with CD1 aggressors over a 10-day defeat protocol (Takahashi et al., 2017). In our study, the attack latency was approximately 100 sec and experimental mice were exposed to aggressive CD1s 60% of the time. Importantly, after we classified mice as being either resilient or susceptible, there were no differences in these variables between these groups which suggests that overall, all mice were exposed to social stress to a similar degree.

In this study, we were able to obtain a greater proportion of resilient mice compared to susceptible mice based on an arbitrary split of their social behaviour. There are limitations to

be acknowledged with this paradigm. Firstly, the social interaction test we used does not assess threat appraisal. A mouse which avoids the CD1 could be doing so as an adaptive response to avoid being attacked any further, even though the CD1 is inside a cage. Conversely, a mouse which we define as resilient could suggest that the chronic stress exposure has impaired its ability to assess threat and act defensively. Future studies could overcome this limitation by using a stimulus mouse of a similar strain or extracting other variables from the existing test such as the approach and flight index (Henriques-Alves and Queiroz, 2016). Secondly, we did not perform any other behavioural tests for depressive- or anxiety-like behaviours. Previous reports have reported a divergence in anxiety-like behaviour in the elevated plus maze between resilient and susceptible mice but reported no differences in the forced swim test or the sucrose preference test (Hammels et al., 2015; Henriques-Alves and Queiroz, 2016; Laine et al., 2018). It is also worth highlighting the work by Krishnan et al., (2007) who examined behaviours for several weeks after the last defeat and reported that of all the behaviours they analysed, only social behaviour remained significantly different between resilient and susceptible mice at the later time point (39 days after the last defeat session). Nevertheless, there are other tests which could be used such as assessing reward function with the intracranial self-stimulation (Der-Avakian et al., 2014). Furthermore, calculating behavioural Z-scores derived from multiple tests may provide more reliable indices of resilience and susceptibility as opposed to a single measurement of social avoidance behaviour. Lastly, we did not characterise any non-social behaviours such as grooming and freezing which could confound interpretation of data from the social interaction test (Meshalkina and Kalueff, 2016). In terms of locomotor activity, as previously observed a social stimulus (CD1 mouse) decreased locomotor activity in all mice (Savignac et al., 2011).

We observed significant elevation of plasma CORT and increased adrenal gland weight only in susceptible mice. Furthermore, there was a significant association between plasma CORT and social interaction behaviour. We speculate that this may reflect dysregulation of HPA-axis, altering it's 'set-point' activity and this may be underscored by differential expression of *Crf* in structures such as the PFC (see below) (Sandi and Haller, 2015). Interestingly, our findings are in contrast with earlier work by Krishan et al., (2007) who reported no differences in plasma CORT between resilient and mice on the day after the last defeat (day 11). However, they did observe a paradoxical increase in plasma CORT in resilient mice and a decrease in susceptible mice weeks later (day 39). Analysis of plasma samples from multiple time points including those taken during the defeat protocol itself may provide further insights into the relationship between stress-induced dysregulation of HPA-axis and behavioural responses to stress (Koolhaas et al., 1999).

There was a decrease in the body weight gain of all stressed mice which has been reported in another study which also used the chronic social defeat stress protocol (Iñiguez et al., 2014). While a significant reduction was observed only the resilient mice, increasing the sample size may have led to a similarly significant effect in the susceptible mice also. This phenotype has been directly linked to elevations of glucocorticoids and leptin, the anorexigenic hormone which inhibits food intake (Maniam and Morris, 2012). Between resilient and susceptible mice, evidence for differential effects of social defeat stress on body weight is equivocal with studies reporting no difference (Bosch-Bouju et al., 2016; Tse et al., 2014), a decrease only in susceptible mice (Krishnan et al., 2007) and an increase in mice which were initially identified as dominant in a hierarchy but subsequently classified as susceptible following defeat stress (Larrieu et al., 2017).

There was an overall increase in spleen weight for all stressed mice. These effects have been shown previously using social defeat stress; (Avitsur et al., 2007; Niraula et al., 2018; Tarr et al., 2012; Wohleb et al., 2014). In the spleen, the mechanisms underpinning stress-induced morphological changes involve increased mobilisation of leukocytes and accumulation of bone-marrow derived hematopoietic progenitors (Jiang et al., 2017; McKim et al., 2018; Wohleb et al., 2014). There was a trend towards an attenuating effect of stress on thymus weight which may have crossed the threshold for significance with a large sample size. In particular, there was a signficant reduction in resilient mice compared to controls. This effect of stress has been previously reported (Hartmann et al., 2012; Schmidt et al., 2007) and could be underpinned by thymocyte apoptosis and effects on thymocyte cellularity (Živković et al., 2005). Given that we observed no differences in thymus or spleen weight between resilient and susceptible mice, we speculate on their relevance to effects on social avoidance behaviour. However, it is possible that the rate of resolution from the inflammatory state resulting from thymic hypotrophy and splenic hypertrophy could be linked to longer-term differences in behavioural outcomes between these two groups of mice.

Given its role in cognition, executive functioning and regulation of the HPA-axis, the functional flexibility of the PFC is a critical determinant of the response to chronic stress exposure (Arnsten, 2009). Indeed, recent clinical imaging studies have shown correlations between stress-coping strategies and PFC plasticity (Sinha et al., 2016). Our data appears to suggest that PFC *Crf* expression in particular has a role in this context with mRNA expression being significantly increased in susceptible mice compared to resilient mice. Interestingly, the temporal effects of the social defeat stress paradigm on *Crf* receptor expression appear to be important; whereas we observed no effects of chronic defeat stress on PFC *Crfr1* mRNA

expression, another study using acute social defeat stress showed increased expression and this underscored deficits in cognitive behaviours (Uribe-Mariño et al., 2016). Future studies will be required to explore the precise downstream molecular effects of PFC *Crf* expression in the context of social behaviour. One approach would be to examine interactions between *Crf* and the *Crf* binding protein (BP), which acts in cell-specific manner (Ketchesin et al., 2017). Another would be to examine the functional role of *Crf in* neuronal responses in the PFC and PFC-driven coherence with other structures in light of recent evidence showing that PFC reactivity and connectivity with the amygdala is differerentially affected between resilient and susceptible mice (Hultman et al., 2016; Kumar et al., 2014).

In our study, there was a stress-induced increase in *Crfr1* mRNA expression in the hippocampus of resilient mice. Previous work has reported that chronic early-life stress and chronic restraint stress in mice induced a reduction in spine density in hippocampal pyramidal neurons, an effect dependent on the expression of *Crfr1* receptors (Chen et al., 2008; Ivy et al., 2010). Moreover, *Crfr1* receptors in the hippocampus have been shown to facilitate induction of long-term potentiation (LTP) (Schierloh et al., 2007). With respect to the lack of differences in the postsynaptic response (I/O curves) recorded in this study, it has to be noted that neither chronic early-life stress nor administration of *Crf* to acute hippocampal brain slices showed any effect on fEPSP amplitude when fEPSPs were obtained through stimulation of Schaffer Collaterals (Ivy et al., 2010; Kratzer et al., 2013). However, one study has shown that if fEPSPs in CA1 were obtained through stimulation of CA3 pyramidal cells, acute administration of *Crf* increased fEPSP amplitude (Kratzer et al., 2013). These findings might explain why we did not see group differences in the postsynaptic response recordings, as fEPSPs in CA1 were evoked through stimulation of Schaffer Collaterals (SC).

Our data suggests that the upregulation of hippocampal *Crfr1* and any consequent changes in synaptic plasticity do not mediate differences in social behaviour but possibly other hippocampal dependent-behaviours such as working or spatial memory. In this regard, we noticed stimulus intensity- and interpulse interval (IPI)-dependent effects on the hippocampal PPR ratio as a measurement of the probability of presynaptic neurotransmitter release. A ratio below 1 (PPD) indicates presynaptic terminals with a high probability of transmitter release upon stimulation, while a ratio above 1 (PPF) indicates a low release probability. At lower stimulation intensities and IPIs of both 25ms and 50ms, we observed a trends towards reductions in PPF in stressed mice. Similar findings have been reported in rats which experienced chronic restraint stress, namely dentate granule cells of stressed rats displayed lower PPR than those of control animals (Radahmadi et al., 2014) using a stimulation strength of 40%, which is inbetween our low intensity stimulation (30%) and our high intensity stimulation (50%). When recruiting more inputs onto CA1 pyramidal cells through higher stimulation intensity and at both IPI of 100ms and 200ms, the PPF of stress-resilient mice was reduced, particularly compared to control mice. This effect seemed to have been driven by the reduction of PPF in stress-resilient mice, although it only trended towards significance. In a previous study, rats which were classified as susceptible to a chronic mild stress protocol expressed PPF of inhibitory postsynaptic currents and accordingly decreased spontaneous GABA-ergic neurotransmission in the dentate gyrus of the ventral hippocampus, while both control and resilient rats expressed PPD (Nieto-Gonzalez et al., 2015), suggesting altered GABA innervation in stress-susceptible rats. Interestingly, excitatory synapses with low release probability (i.e., PPF) together with feed-forward inhibitory synapses in the rat hippocampus function as a high-pass filter (Klyachko and Stevens, 2006).

In this context, the term high-pass filter refers to a synapse that works at a state of low synaptic strength when it is stimulated with low frequency discharges, but switches to a state of hightened synaptic strength as a response to high frequency stimulation that exceeds a certain frequency threshold (i.e. its cut-off frequency). Synapses characterized by low transmitter release probability (i.e., PPF) are particularly suited to fulfill this function, as a low-frequency stimulation of these synapses would result only in a weak postsynaptic response, whereas high-frequency stimulation would result in a much stronger postsynaptic response, expressed as the increased fEPSP after the second pulse in our PPR recordings. Unfortunately, our experiment was not set-up to determine if potential differences in PPF between stressed and control mice would stem from an underlying alteration of the filter function of the SC-CA1 synapse, e.g. by determining the cut-off frequency (i.e. the stimulation frequency that needs to be exceeded to cause a strong postsynaptic response, which would contribute to LTP expression in CA1). However, in rodent hippocampal slices, it has been demonstrated that an increase in release probability (i.e. a reduction in PPF) contributes to LTP expression (Madroñal et al., 2009; Schulz, 1997). Generally, inescapable stress attenuates LTP expression, while enhancing the expression of LTD (Kim and Diamond, 2002; Richter-Levin and Xu, 2018). This has been confirmed recently for chronic social defeat stress in both mice and Chinese tree shrews (Wang et al., 2013; Yang et al., 2018). In light of the inverse relationship between PPF and LTP described above, our results seemingly contradict these findings. We mainly observed a reduction of PPF in stress resilient mice at lower stimulation intensity at 50ms IPI, while the reduction at the 25ms IPI trended towards significance. At higher stimulation intensity, the trend towards a reduction in PPF at 100ms and 200ms IPI appeared to be driven by reduction in stress-resilient mice. However, Yang et al., (2018) also reported a concomitant reduction of NMDA-mediated currents in CA1 pyramidal cells of

stress-susceptible mice compared to controls, which plays an important role for the observed reduction in LTP. Unfortunately, Yang et al. excluded stress-resilient mice from their study.

We were not able to attribute certain changes of CA1 PPF clearly to either stress-susceptible or stress-resilient mice. Thus, both stress phenotypes do not differ in their functioning of presynaptic release probability, but instead display reduced PPF at different IPIs and stimulus intensities tested. While generally the reduction of PPF positively correlates with LTP expression in the hippocampus, chronic social defeat stress appears to affect LTP not via a presynaptic route, but rather through a postsynaptic mechanism, involving the reduction of NMDAR-mediated currents (Yang et al., 2018). Nevertheless, our results contribute to the growing body of evidence of distinctly affected hippocampal synaptic physiology in both mice susceptible or resilient to chronic social defeat stress. The main limitation of our study is the small sample size, which did not permit us to examine the effects of chronic social defeat stress on synaptic physiology in more depth. Thus, in order to unravel whether stress-resilient mice posess a particular predisposition in their synaptic physiology and/or plasticity leaving their behavioural faculties unscathed as opposed to stress-susceptible, more extensive studies are needed.

The BNST and amygdala are linked structures both of which are stress-sensitive and implicated in regulation of social behaviour (Duque-Wilckens et al., 2018; Volk et al., 2014). However, they are both made up of several subregions; the BNST in particular is known to have at least 20 (Lebow and Chen, 2016). As such, gross-dissection is likely to have produced diluted signals that may not be entirely informative. Future studies will need to consider using high-resolution analysis of these structures in sub-regions. For example, it has been shown

that there is differential expression of enkephalin in the basolateral amygdala of mice following social defeat stress (Henry et al., 2018). Similary, chronic unpredictable stress exposure in rats has resulted in sub-region specific effects on expression of *Crfr1*, *Crfr2*, GABA receptor A and NMDA receptor subunit 2B in the BNST (Ventura-Silva et al., 2012). Lastly, it must also be noted that the BNST is a sexually dimorphic structure (Lebow and Chen, 2016); we did not examine females but it is likely that gene expression profiles would significantly differ in response to female-specific chronic social defeat stress paradigms (Harris et al., 2018; Takahashi et al., 2017).

Neuroinflammation is one of the features of stress-induced psychopathologies in subsets of patients and this phenomenon has been observed in preclinical studies using the social defeat stress paradigm (Weber et al., 2017). For example, a recent study has shown increased activation of the peripheral innate immune system (Menard et al., 2017). Another, has reported that the release of inflammatory monocytes from the bone marrow into the blood is linked to social defeat stress-induced release of plasma corticosterone (Niraula et al., 2018). Interestingly, we observed a significant increase in the proportion of inflammatory monocytes in the blood of susceptible mice relative to controls. Trafficking of inflammatory monocytes from the periphery into the brain and differentiation into macrophages precedes the onset of neuroinflammation mediated by the activation of microglia and release of pro-inflammatory cytokines (Wohleb et al., 2015). Cytokine-induced dysregulation of serotonergic and dopaminergic neurotransmission, increased glutamate-mediated excitotoxicity and reduced neurogenesis may be linked to the decrease in social behaviour in susceptible mice (Stein et al., 2017).

Expression of MHC-II classically represents an activation marker on granulocytes (Lin and Loré, 2017) and monocytes (Bunbury et al., 2008) which subsequently facilitates activation of T-cells. However, glucocorticoids can also regulate the expression of MHC-II. We identified a trend towards decreased MHC-II expression on inflammatory monocytes in susceptible mice; increasing the sample size may have led to the detection of significance for this group. This decrease might be explained by the increase in corticosterone levels, as glucocorticoids have previously been shown to decrease MHC-II gene expression on monocytes (Achuthan et al., 2018; van de Garde et al., 2014). Our inflammatory monocyte data may indicate that these cells are more affected by stress in susceptible mice, compared to resilient mice. We also report a significant increase in the prevalence of granulocytes for stressed mice which is consistent with the literature (Wohleb et al., 2015). However, CD11b receptor expression on monocytes and granulocytes remains unaffected by defeat stress. Notwithstanding our findings, we acknowledge that one of the limitations of our analysis is the absence of data on whether the peripheral immune changes we report here are associated with specific altered expression of neuroimmune markers in the brain.

In summary, this report provides an overview of the differential impact that our chronic social defeat stress paradigm has on a range of central and peripheral parameters associated with behavioural stress-resilience and stress-susceptibility. Our most striking findings are the increased inflammatory circulating monocytes, plasma corticosterone, adrenal hypertrophy, increased PFC *Crf* mRNA expression in stress-susceptible mice and differential hippocampal synaptic plasticity. Future studies will identify the mechanisms via which these changes impact on behaviour and examine their viability as therapeutic targets to treat stress-induced psychopathologies and to facilitate resilience against future stress exposure.

Declarations:

Acknowledgements:

The authors would like to thank Dr Kieran Rea and Dr Kenneth O'Riordan for helpful comments on the manuscript and Mr. Patrick Fitzgerald and Ms Collette Manley for technical assistance with animal husbandry. The authors would also like to thank Dr Panagiota Stamou for her assistance and advice with flow cytometry

Funding:

This research was funded by a Marie-Sklowdowska-Curie Actions Individual Fellowship to AG from the European Research Council (Grant Number 704995) and conducted in the APC Microbiome Institute, which is funded by Science Foundation Ireland (SFI; grant nos. SFI/12/RC/2273). MB is supported by an educational grant from Science Foundation Ireland (SFI), Ireland (15/JP-HDHL/3270; JPI-HDHL-NutriCog project 'AMBROSIAC'). TGD and JFC are also supported by the Irish Health Research Board, the Dept. of Agriculture, Food and the Marine and Enterprise Ireland. TGD and JFC are the principal investigators in the APC Microbiome Institute, University College Cork. The authors declare that they have no competing interests. The funders had no role in study design, data collection and interpretation, or the decision to submit the work for publication. The APC Microbiome Institute conducts research funded by many pharmaceutical and food companies. TGD has been an invited speaker at meetings organized by Servier, Lundbeck, Janssen and AstraZeneca and has received research funding from Mead Johnson, Cremo, Suntory Wellness, Nutricia and 4D Pharma. JFC has been an invited speaker at meetings organized by Mead Johnson, Yakult, Alkermes and Janssen and has received research funding from Mead Johnson, Cremo, Suntory Wellness, Nutricia and 4D Pharma.

Availability of data and materials:

All data generated or analysed during this study are included in this published article.

Author contributions:

AG and JFC designed the study. AG managed the project and carried out all stress procedures and behavioural experiments. MB and MVDW performed flow cytometry on trunk blood samples. TB and ROC performed hippocampal electrophysiology. APV assisted with collection of brain tissue samples. JML analysed spleen and thymus morphology. BM and GM assisted with analysis of gene expression and plasma corticosterone. AG, TB and TFSB carried out statistical analysis. AG analysed the data and co-wrote the manuscript. TGD and JFC provided supervision. All authors contributed to the interpretation of the data, critically revised the manuscript, read and approved the final version before submission.

Ethics approval and consent to participate:

All experiments were conducted in accordance with European Directive 86/609/EEC, Recommendation 2007/526/65/EC, and approved by the Health Products Regulatory Authority (AE19130-P031) as well as the Animal Experimentation Ethics Committee of University College Cork. All efforts were made to minimise animal suffering and to reduce the number of animals used.

References

Achuthan, A., et al., 2018. Glucocorticoids promote apoptosis of proinflammatory monocytes by inhibiting ERK activity. Cell Death Dis 9, 267.

Ambrée, O., et al., 2018. Alterations of the Innate Immune System in Susceptibility and Resilience After Social Defeat Stress. Front Behav Neurosci 12, 141.

Arnsten, A.F.T., 2009. Stress signalling pathways that impair prefrontal cortex structure and function. Nat Rev Neurosci 10, 410-422.

Avitsur, R., et al., 2007. Subordinate Social Status Modulates the Vulnerability to the Immunological Effects of Social Stress. Psychoneuroendocrinology 32, 1097-1105.

Bosch-Bouju, C., et al., 2016. Endocannabinoid-Mediated Plasticity in Nucleus Accumbens Controls Vulnerability to Anxiety after Social Defeat Stress. Cell Rep 16, 1237-1242.

Bunbury, A., et al., 2008. Functional analysis of monocyte MHC class II compartments. FASEB J 23, 164-171.

Burokas, A., et al., 2017. Targeting the Microbiota-Gut-Brain Axis: Prebiotics Have Anxiolytic and Antidepressant-like Effects and Reverse the Impact of Chronic Stress in Mice. Biol Psychiatry 82, 472-487.

Chen, Y., et al., 2008. Rapid Loss of Dendritic Spines after Stress Involves Derangement of Spine Dynamics by Corticotropin-Releasing Hormone. J Neurosci 28, 2903-2911.

Der-Avakian, A., et al., 2014. Enduring deficits in brain reward function after chronic social defeat in rats: susceptibility, resilience, and antidepressant response. Biol Psychiatry 76, 542-549.

Duque-Wilckens, N., et al., 2018. Oxytocin Receptors in the Anteromedial Bed Nucleus of the Stria Terminalis Promote Stress-Induced Social Avoidance in Female California Mice. Biol Psychiatry 83, 203-213.

Franklin, Tamara B., et al., 2012. Neural Mechanisms of Stress Resilience and Vulnerability. Neuron 75, 747-761.

Ginhoux, F., Jung, S., 2014. Monocytes and macrophages: developmental pathways and tissue homeostasis. Nat Rev Immunol 14, 392-404.

Hammels, C., et al., 2015. Differential susceptibility to chronic social defeat stress relates to the number of Dnmt3a-immunoreactive neurons in the hippocampal dentate gyrus. Psychoneuroendocrinology 51, 547-556.

Harris, A.Z., et al., 2018. A Novel Method for Chronic Social Defeat Stress in Female Mice. Neuropsychopharmacology 43, 1276-1283.

Hartmann, J., et al., 2012. The involvement of FK506-binding protein 51 (FKBP5) in the behavioral and neuroendocrine effects of chronic social defeat stress. Neuropharmacology 62, 332-339.

Hasegawa, K., et al., 2018. Sevoflurane inhibits presynaptic calcium influx without affecting presynaptic action potentials in hippocampal CA1 region. Biomed Res 39, 223-230.

Henriques-Alves, A.M., Queiroz, C.M., 2016. Ethological Evaluation of the Effects of Social Defeat Stress in Mice: Beyond the Social Interaction Ratio. Front Behav Neurosci 9, 364.

Henry, M.S., et al., 2018. Delta Opioid Receptor Signaling Promotes Resilience to Stress Under the Repeated Social Defeat Paradigm in Mice. Front Mol Neurosci 11, 100.

Hinds, H.L., et al., 2003. Essential function of alpha-calcium/calmodulin-dependent protein kinase II in neurotransmitter release at a glutamatergic central synapse. Proc Natl Acad Sci U S A 100, 4275-4280.

Hultman, R., et al., 2016. Dysregulation of Prefrontal Cortex-Mediated Slow-Evolving Limbic Dynamics Drives Stress-Induced Emotional Pathology. Neuron 91, 439-452.

Iñiguez, S.D., et al., 2014. Social defeat stress induces a depression-like phenotype in adolescent male c57BL/6 mice. Stress 17, 247-255.

Ivy, A.S., et al., 2010. Hippocampal dysfunction and cognitive impairments provoked by chronic early-life stress involve excessive activation of CRH receptors. J Neurosci 30, 13005-13015.

Jiang, W., et al., 2017. Spleen contributes to restraint stress induced changes in blood leukocytes distribution. Sci Rep 7, 6501.

Jochems, J., et al., 2015. Enhancement of stress resilience through histone deacetylase 6-mediated regulation of glucocorticoid receptor chaperone dynamics. Biol Psychiatry 77, 345-355.

Kentner, A.C., et al., 2018. Resilience priming: Translational models for understanding resiliency and adaptation to early life adversity. Dev Psychobiol In press.

Ketchesin, K.D., et al., 2017. Cell Type-Specific Expression of Corticotropin-Releasing Hormone-Binding Protein in GABAergic Interneurons in the Prefrontal Cortex. Front Neuroanat 11, 90.

Kim, J.J., Diamond, D.M., 2002. The stressed hippocampus, synaptic plasticity and lost memories. Nat Rev Neurosci 3, 453-462.

Klyachko, V.A., Stevens, C.F., 2006. Excitatory and Feed-Forward Inhibitory Hippocampal Synapses Work Synergistically as an Adaptive Filter of Natural Spike Trains. PLoS Biology 4, e207.

Koolhaas, J.M., et al., 1999. Coping styles in animals: current status in behavior and stress-physiology. Neuroscience & Biobehavioral Reviews 23, 925-935.

Kratzer, S., et al., 2013. Activation of CRH receptor type 1 expressed on glutamatergic neurons increases excitability of CA1 pyramidal neurons by the modulation of voltage-gated ion channels. Front Cell Neurosci 7, 91.

Krishnan, V., et al., 2007. Molecular Adaptations Underlying Susceptibility and Resistance to Social Defeat in Brain Reward Regions. Cell 131, 391-404.

Kumar, S., et al., 2014. Prefrontal cortex reactivity underlies trait vulnerability to chronic social defeat stress. Nat Commun 5, 4537.

Laine, M.A., et al., 2018. Genetic Control of Myelin Plasticity after Chronic Psychosocial Stress. Eneuro 5, e0166-0118.2018 0161-0116.

Larrieu, T., et al., 2017. Hierarchical Status Predicts Behavioral Vulnerability and Nucleus Accumbens Metabolic Profile Following Chronic Social Defeat Stress. Curr Biol 27, 2202-2210.

Lebow, M.A., Chen, A., 2016. Overshadowed by the amygdala: the bed nucleus of the stria terminalis emerges as key to psychiatric disorders. Mol Psychiatry 21, 450-463.

Lessard, A.-J., et al., 2017. Triggering of NOD2 Receptor Converts Inflammatory Ly6C-high into Ly6C-low Monocytes with Patrolling Properties. Cell Rep 20, 1830-1843.

Lin, A., Loré, K., 2017. Granulocytes: New Members of the Antigen-Presenting Cell Family. Front Immunol 8, 1781.

Madroñal, N., et al., 2009. Differing presynaptic contributions to LTP and associative learning in behaving mice. Front Behav Neurosci 3, 7.

Maniam, J., Morris, M.J., 2012. The link between stress and feeding behaviour. Neuropharmacology 63, 97-110.

McKim, D.B., et al., 2018. Social Stress Mobilizes Hematopoietic Stem Cells to Establish Persistent Splenic Myelopoiesis. Cell Rep 25, 2552-2562.

Menard, C., et al., 2017. Social stress induces neurovascular pathology promoting depression. Nat Neurosci 20, 1752-1760.

Meshalkina, D.A., Kalueff, A.V., 2016. Commentary: Ethological Evaluation of the Effects of Social Defeat Stress in Mice: Beyond the Social Interaction Ratio. Front Behav Neurosci 10, 155.

Motulsky, H.J., Brown, R.E., 2006. Detecting outliers when fitting data with nonlinear regression – a new method based on robust nonlinear regression and the false discovery rate. BMC Bioinformatics 7, 123.

Nieto-Gonzalez, J.L., et al., 2015. Presynaptic Plasticity as a Hallmark of Rat Stress Susceptibility and Antidepressant Response. PLoS One 10, e0119993.

Niraula, A., et al., 2018. Corticosterone Production during Repeated Social Defeat Causes Monocyte Mobilization from the Bone Marrow, Glucocorticoid Resistance, and Neurovascular Adhesion Molecule Expression. J Neurosci 38, 2328-2340.

Petersen, R.P., et al., 2013. Electrophysiological identification of medial and lateral perforant path inputs to the dentate gyrus. Neuroscience 252, 154-168.

Pfau, M.L., Russo, S.J., 2015. Peripheral and central mechanisms of stress resilience. Neurobiol Stress 1, 66-79.

Pryce, C.R., Fuchs, E., 2017. Chronic psychosocial stressors in adulthood: Studies in mice, rats and tree shrews. Neurobiol Stress 6, 94-103.

Radahmadi, M., et al., 2014. Effect of chronic stress on short and long-term plasticity in dentate gyrus; study of recovery and adaptation. Neuroscience 280, 121-129.

Richter-Levin, G., Xu, L., 2018. How could stress lead to major depressive disorder? IBRO Rep 4, 38-43.

Sandi, C., Haller, J., 2015. Stress and the social brain: behavioural effects and neurobiological mechanisms. Nat Rev Neurosci 16, 290-304.

Savignac, H.M., et al., 2011. Increased sensitivity to the effects of chronic social defeat stress in an innately anxious mouse strain. Neuroscience 192, 524-536.

Schierloh, A., et al., 2007. Corticotropin-releasing factor (CRF) receptor type 1-dependent modulation of synaptic plasticity. Neurosci Lett 416, 82-86.

Schmidt, M.V., et al., 2007. Persistent neuroendocrine and behavioral effects of a novel, etiologically relevant mouse paradigm for chronic social stress during adolescence. Psychoneuroendocrinology 32, 417-429.

Schulz, P.E., 1997. Long-term potentiation involves increases in the probability of neurotransmitter release. Proc Natl Acad Sci U S A 94, 5888-5893.

Sinha, R., et al., 2016. Dynamic neural activity during stress signals resilient coping. Proc Natl Acad Sci USA 113, 8837.

Slattery, D.A., Cryan, J.F., 2017. Modelling depression in animals: at the interface of reward and stress pathways. Psychopharmacology 234, 1451-1465.

Stein, D.J., et al., 2017. Microglial Over-Activation by Social Defeat Stress Contributes to Anxiety- and Depressive-Like Behaviors. Front Behav Neurosci 11, 207.

Stilling, R.M., et al., 2018. Social interaction-induced activation of RNA splicing in the amygdala of microbiome-deficient mice. eLife 7, e33070.

Takahashi, A., et al., 2017. Establishment of a repeated social defeat stress model in female mice. Sci Rep 7, 12838.

Tarr, A.J., et al., 2012. β-Adrenergic receptor mediated increases in activation and function of natural killer cells following repeated social disruption. Brain Behav Immun 26, 1226-1238.

Tse, Y.C., et al., 2014. A longitudinal study of stress-induced hippocampal volume changes in mice that are susceptible or resilient to chronic social defeat. Hippocampus 24, 1120-1128.

Uribe-Mariño, A., et al., 2016. Prefrontal Cortex Corticotropin-Releasing Factor Receptor 1 Conveys Acute Stress-Induced Executive Dysfunction. Biol Psychiatry 80, 743-753.

van de Garde, M.D.B., et al., 2014. Chronic Exposure to Glucocorticoids Shapes Gene Expression and Modulates Innate and Adaptive Activation Pathways in Macrophages with Distinct Changes in Leukocyte Attraction. J Immunol, 1302138.

Ventura-Silva, A.P., et al., 2012. Stress shifts the response of the bed nucleus of the stria terminalis to an anxiogenic mode. Eur J Neurosci 36, 3396-3406.

Volk, N., et al., 2014. MicroRNA-19b Associates with Ago2 in the Amygdala Following Chronic Stress and Regulates the Adrenergic Receptor Beta 1. J Neurosci 34, 15070.

Wang, J., et al., 2013. Chronic clomipramine treatment reverses core symptom of depression in subordinate tree shrews. PLoS One 8, e80980.

Weber, M.D., et al., 2017. Repeated Social Defeat, Neuroinflammation, and Behavior: Monocytes Carry the Signal. Neuropsychopharmacology 42, 46-61.

WHO, 2017. Depression and Other Common Mental Disorders: Global Health Estimates. In: Organisation, W.H. (Ed.).

Wohleb, E.S., et al., 2014. Re-establishment of Anxiety in Stress-Sensitized Mice Is Caused by Monocyte Trafficking from the Spleen to the Brain. Biol Psychiatry 75, 970-981.

Wohleb, E.S., et al., 2015. Monocyte trafficking to the brain with stress and inflammation: a novel axis of immune-to-brain communication that influences mood and behavior. Front Neurosci 8, 447-447.

Wu, L.G., Saggau, P., 1994. Presynaptic calcium is increased during normal synaptic transmission and paired-pulse facilitation, but not in long-term potentiation in area CA1 of hippocampus. J Neurosci 14, 645-654.

Yang, Y., et al., 2018. Effect of Ketamine on LTP and NMDAR EPSC in Hippocampus of the Chronic Social Defeat Stress Mice Model of Depression. Front Behav Neurosci 12, 229.

Živković, I.P., et al., 2005. Exposure to forced swim stress alters morphofunctional characteristics of the rat thymus. J Neuroimmunol 160, 77-86.

Zorn, J.V., et al., 2017. Cortisol stress reactivity across psychiatric disorders: A systematic review and meta-analysis. Psychoneuroendocrinology 77, 25-36.

Figure Legends:

Figure 1 - Experimental timeline.

Figure 2: **Chronic social defeat stress induces phenotypes associated with stress-resilience and stress-susceptibility. (a)** Social interaction behaviour. *vs. control*, *@p<0.05*, *#p<0.01; vs. susceptible*, **p<0.001*. SIT-social interaction ratio. **(b)** Locomotor activity. Trial 1- *vs. control*, *@p<0.05*. Trial 2-*vs. Trial 1 control*, **p<0.001; vs. Trial 1 susceptible*, *#p<0.01; vs Trial 1 resilient*, *#p<0.01*. **(c)** Plasma corticosterone (CORT) levels at baseline and at the end of the stress protocol. *vs. control and resilient*, *#p<0.01*. **(d)** PERMANOVA correlation plot for social behaviour vs. plasma CORT. **(e)** Change in body weight. *vs. control*, *@p<0.05*. **(f)** Weight of adrenals as a percentage of body weight (BW) *vs. control*, *@p<0.05; vs. susceptible*, *$p<0.05*. **(g)** Weight of thymus as a percentage of body weight. *vs. control*. *@p<0.05*. **(h)** Weight of spleen as a percentage of body weight. *vs. control*, *#p<0.01*. (a),(b),(e) control = 27, susceptible = 14, resilient = 18. (c),(d),(f)-(h) control = 19-25, susceptible = 10-14, resilient = 11-14. All data are expressed as mean±SEM.

Figure 3: **Effect of chronic psychosocial defeat stress on gene expression (mRNA).** *vs. control*, *@p<0.05*, *vs. susceptible*, **p<0.05*. control=21-22, susceptible=10-11, resilient=9-11. All data are expressed as mean±SEM. Abbreviations: Gr-glucocorticoid receptor, Mr-mineralocorticoid receptor, Crf-corticotropic release factor, Crfr1-corticotropic release factor receptor 1, Crfr2-corticotropic release factor receptor 2, Fkbp5- FK506 binding protein 5, Adycap1-adenylate cyclase activating polypeptide 1, Pac1- Adycap1 receptor.

Figure 4 - **Chronic social defeat stress induces differential effects on hippocampal synaptic plasticity. (a)** Postsynaptic response. fEPSP-field excitatory post synaptic potential. **(b)** Paired-pulse ratio (PPR) at 30% stimulation intensity. **(c)** PPR at 505 stimulation intensity. control=5, susceptible=3, resilient=6, 8-14 slices/group. All data are expressed as mean±SEM.

Figure 5 - **Chronic social defeat stress induces differential effects on the peripheral innate immune system. (a)** For the flow cytometry data analysis, peripheral blood mononuclear cells (PMBCs) were selected based on the forward scatter (FSC) and sideward (SSC). **(b)** Granulocytes were subsequently selected based on the surface expression cluster of differentiation molecule 11b+ (CD11b+), SSC(high), whereas CD11b+, SSC(low) cells were used to identify monocytes. **(c)** Inflammatory monocytes were selected based on high expression of lymphocyte antigen 6 complex (LY6C(high)). **(d)** Percentage of circulating inflammatory monocytes. **(e)** Percentage of resident CD11b+, SSC(low), LY6C(low) cells, consisting of mainly resident monocytes. **(f)** Percentage of major histocompatibility complex class II (MHC-II+) expressing inflammatory monocytes. **(g)** CD11b receptor expression on CD11b+ expressing inflammatory monocytes shown as median fluorescence intensity (MFI). **(h)** Percentage of circulating granulocytes. **(i)** Percentage of MHC-II+ expressing granulocytes. **(j)** CD11b receptor expression on CD11b+ expressing granulocytes. **(k)** The staining intensity of the MHC-II receptor is shown, where an extra staining histogram is added for MHC-II+ control staining, as the percentage MHC-II for the investigated target populations was relatively low. **(l)** The staining intensity of CD11b receptor is shown. *vs. control*, *@p<0.05*. control=19-20, susceptible=6, resilient=11-12. All data are expressed as mean±SEM.

Supplementary Figure 1 – Schematic of the experimental setup to assess social interaction behaviour.

Supplementary Figure 2 – (a) Number of days that CD1 showed aggressive behaviors and (b) average latency to attack or adopt a submissive posture. Control = 27, susceptible = 14, resilient = 18.

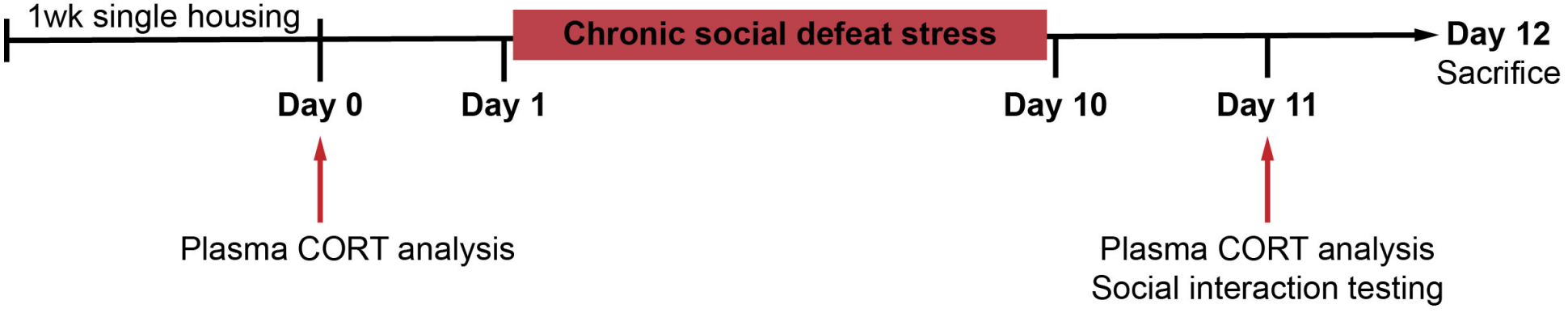
1wk single housing
Chronic social defeat stress
Day 12
Sacrifice
Day 0
Day 1
Day 10
Day 11
Plasma CORT analysis
Plasma CORT analysis
Social interaction testing

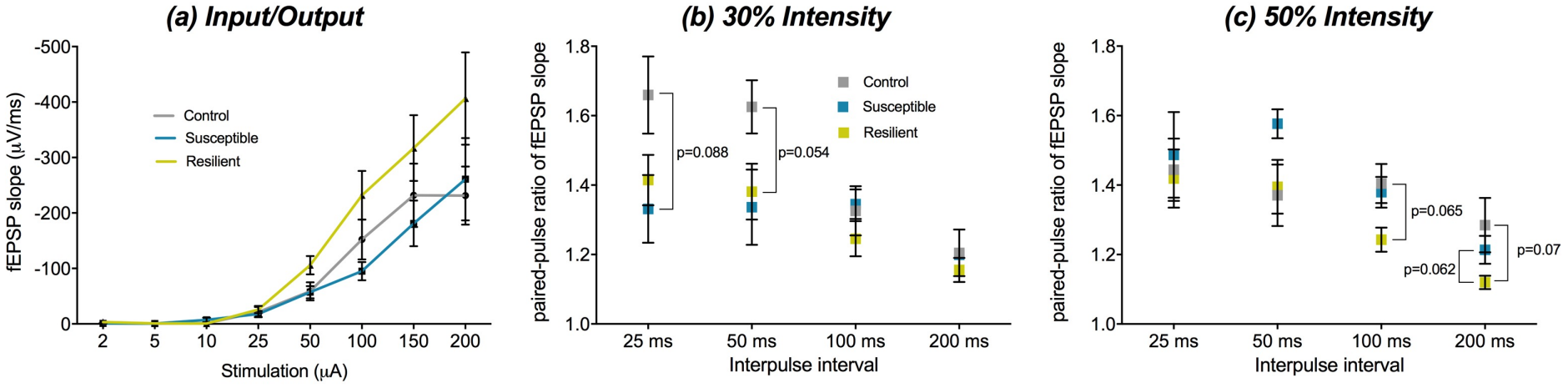
(a) Input/Output
fEPSP slope (μV/ms)
-500
-400
-300
-200
-100
0
Control
Susceptible
Resilient
2
5
10
25
50
100
150
200
Stimulation (μA)
(b) 30% Intensity
paired-pulse ratio of fEPSP slope
1.8
1.6
1.4
1.2
1.0
p=0.088
p=0.054
Control
Susceptible
Resilient
25 ms
50 ms
100 ms
200 ms
Interpulse interval
(c) 50% Intensity
paired-pulse ratio of fEPSP slope
1.8
1.6
1.4
1.2
1.0
p=0.065
p=0.062
p=0.07
25 ms
50 ms
100 ms
200 ms
Interpulse interval

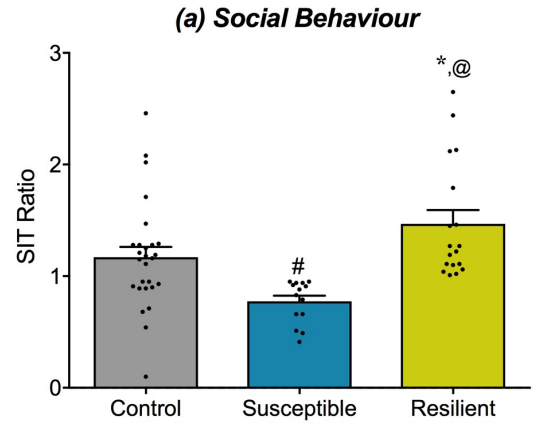
(a) Social Behaviour
SIT Ratio
3
2
1
0
*,@
#
Control
Susceptible
Resilient

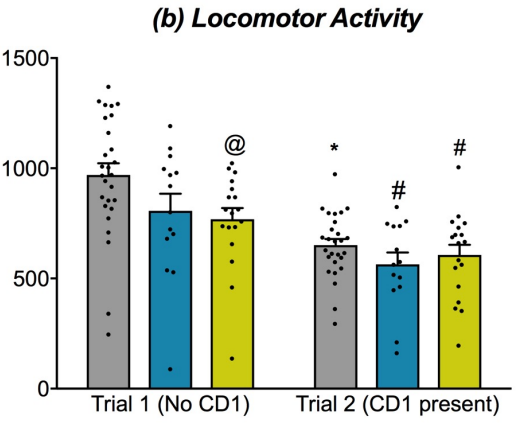
(b) Locomotor Activity
1500
1000
500
0
@
*
#
#
Trial 1 (No CD1)
Trial 2 (CD1 present)

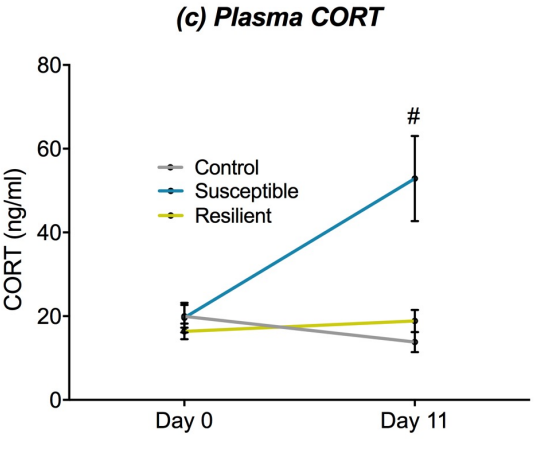
(c) Plasma CORT
CORT (ng/ml)
80
60
40
20
0
#
Control
Susceptible
Resilient
Day 0
Day 11

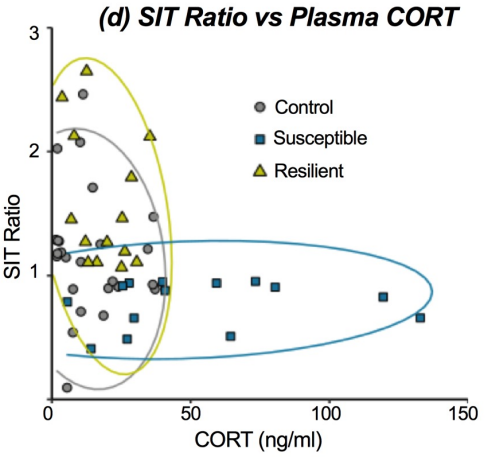
(d) SIT Ratio vs Plasma CORT
SIT Ratio
3
2
1
0
Control
Susceptible
Resilient
0
50
100
150
CORT (ng/ml)

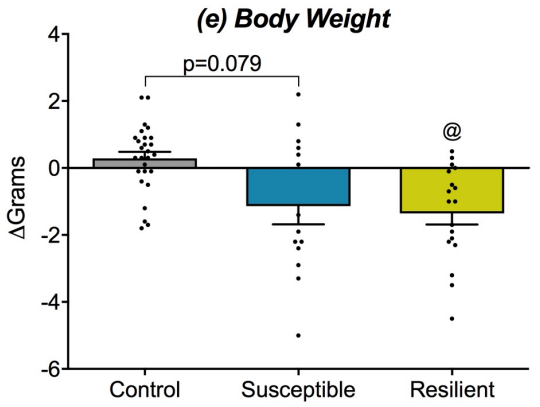
(e) Body Weight
ΔGrams
4
2
0
-2
-4
-6
p=0.079
@
Control
Susceptible
Resilient

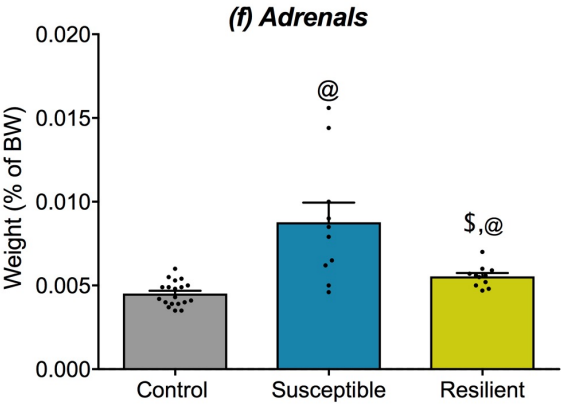
(f) Adrenals
Weight (% of BW)
0.020
0.015
0.010
0.005
0.000
@
$,@
Control
Susceptible
Resilient

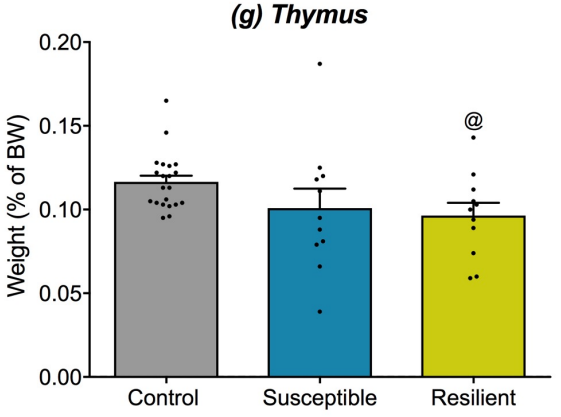
(g) Thymus
Weight (% of BW)
0.20
0.15
0.10
0.05
0.00
@
Control
Susceptible
Resilient

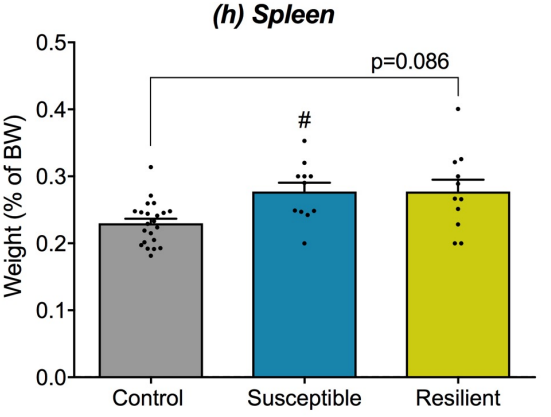
(h) Spleen
Weight (% of BW)
0.5
0.4
0.3
0.2
0.1
0.0
p=0.086
#
Control
Susceptible
Resilient

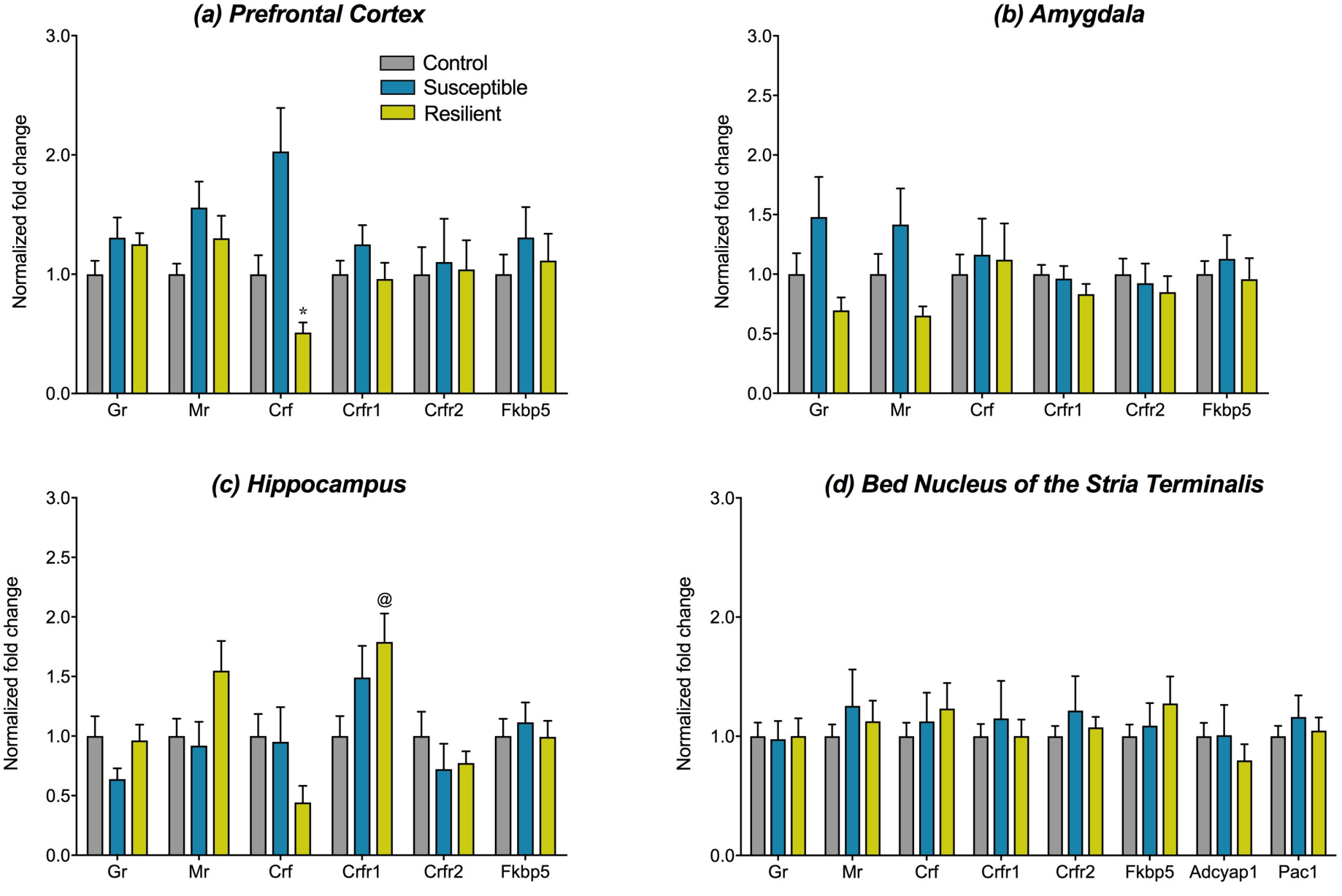
(a) Prefrontal Cortex
Control
Susceptible
Resilient
Normalized fold change
3.0
2.0
1.0
0.0
*
Gr
Mr
Crf
Crfr1
Crfr2
Fkbp5
(b) Amygdala
Normalized fold change
3.0
2.5
2.0
1.5
1.0
0.5
0.0
Gr
Mr
Crf
Crfr1
Crfr2
Fkbp5
(c) Hippocampus
Normalized fold change
3.0
2.5
2.0
1.5
1.0
0.5
0.0
@
Gr
Mr
Crf
Crfr1
Crfr2
Fkbp5
(d) Bed Nucleus of the Stria Terminalis
Normalized fold change
3.0
2.0
1.0
0.0
Gr
Mr
Crf
Crfr1
Crfr2
Fkbp5
Adcyap1
Pac1

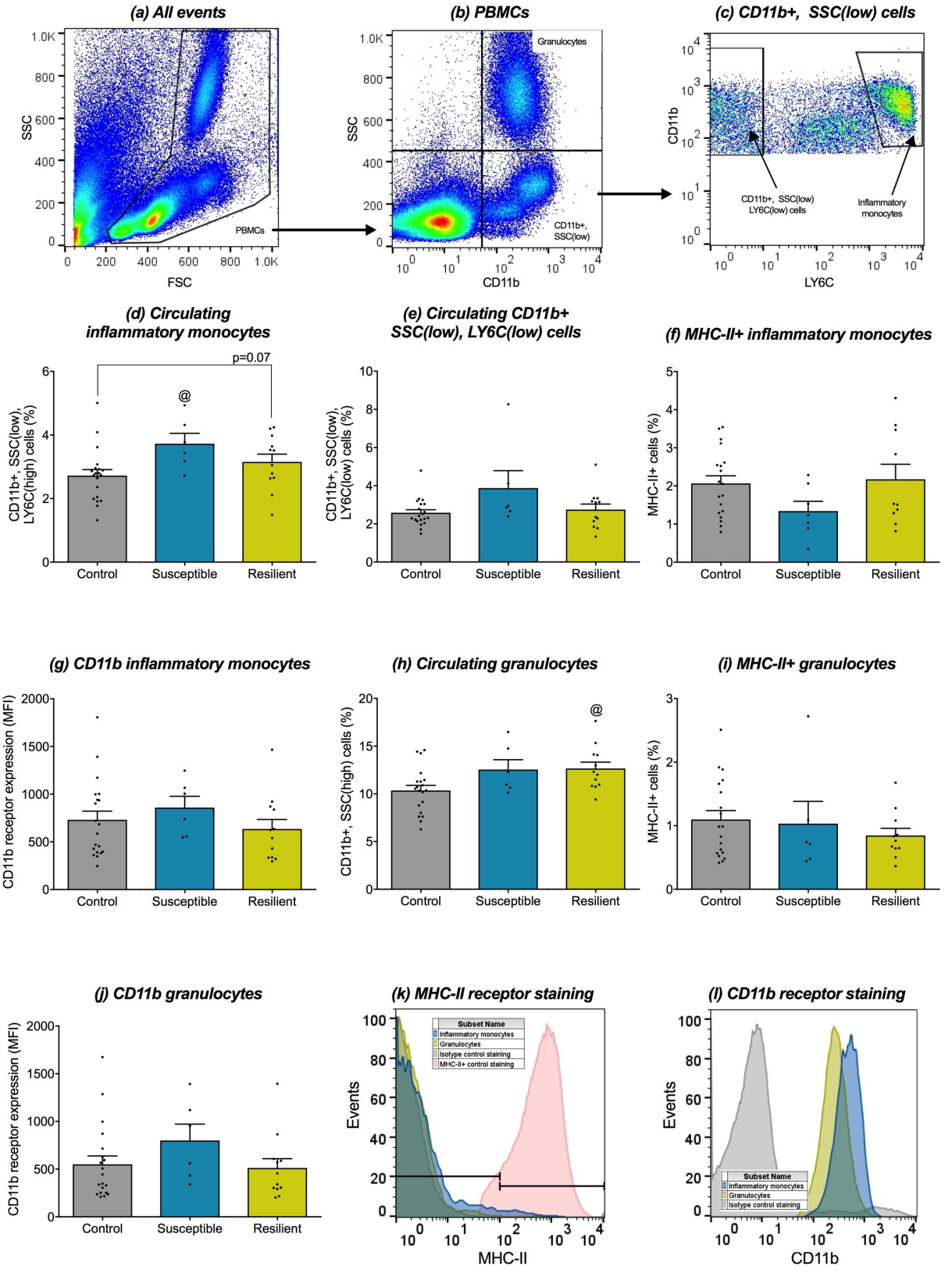
(a) All events
SSC
FSC
PBMCs
(b) PBMCs
Granulocytes
CD11b+, SSC(low)
CD11b
(c) CD11b+, SSC(low) cells
CD11b
LY6C
CD11b+, SSC(low) LY6C(low) cells
Inflammatory monocytes
(d) Circulating inflammatory monocytes
p=0.07
CD11b+, SSC(low), LY6C(high) cells (%)
(e) Circulating CD11b+ SSC(low), LY6C(low) cells
CD11b+, SSC(low), LY6C(low) cells (%)
(f) MHC-II+ inflammatory monocytes
MHC-II+ cells (%)
Control
Susceptible
Resilient
(g) CD11b inflammatory monocytes
CD11b receptor expression (MFI)
(h) Circulating granulocytes
CD11b+, SSC(high) cells (%)
(i) MHC-II+ granulocytes
(j) CD11b granulocytes
(k) MHC-II receptor staining
Subset Name
Inflammatory monocytes
Granulocytes
Isotype control staining
MHC-II+ control staining
Events
MHC-II
(l) CD11b receptor staining

Resilience to Chronic Stress Is Associated with Specific Neurobiological, Neuroendocrine and Immune Responses.

Table 1 – Number of mice in each experimental group used for each analysis

Assay	Control	Susceptible	Resilient
Social behaviour	27	14	~~15~~18
Plasma CORT	25		14
Adrenals weight	19	10	11
Thymus weight	21	11	11
Spleen weight	22	14	14
PCR	~~21~~22	11	11
Electrophysiology	5	3	6
Flow cytometry	20	6	12

Resilience to Chronic Stress Is Associated with Specific Neurobiological, Neuroendocrine and Immune Responses.

Table 2 – qRT-PCR primer assay IDs

Gene	Assay ID
Corticotropin releasing factor (*Crf*)	Mm.PT.58.32061593
Crf receptor 1 (*Crfr1*)	Mm.PT.58.13604366
Crf receptor 2 (*Crfr2*)	Mm.PT.58.12499462
Glucorticoid receptor (*Gr*)	Mm.PT.58.42952901
Mineralocorticoid receptor (*Mr*)	Mm.PT.58.30752774
FK506 binding protein 5 (*Fkbp5*)	Mm.PT.58.45861921
Adenylate cyclase activating peptide (*Adcyap1*)	Mm.PT.58.31241204
Adcyap1 receptor 1 (*Pac1*)	Mm.PT.58.32800544
β-actin	Mm.PT.39a.22214843.g

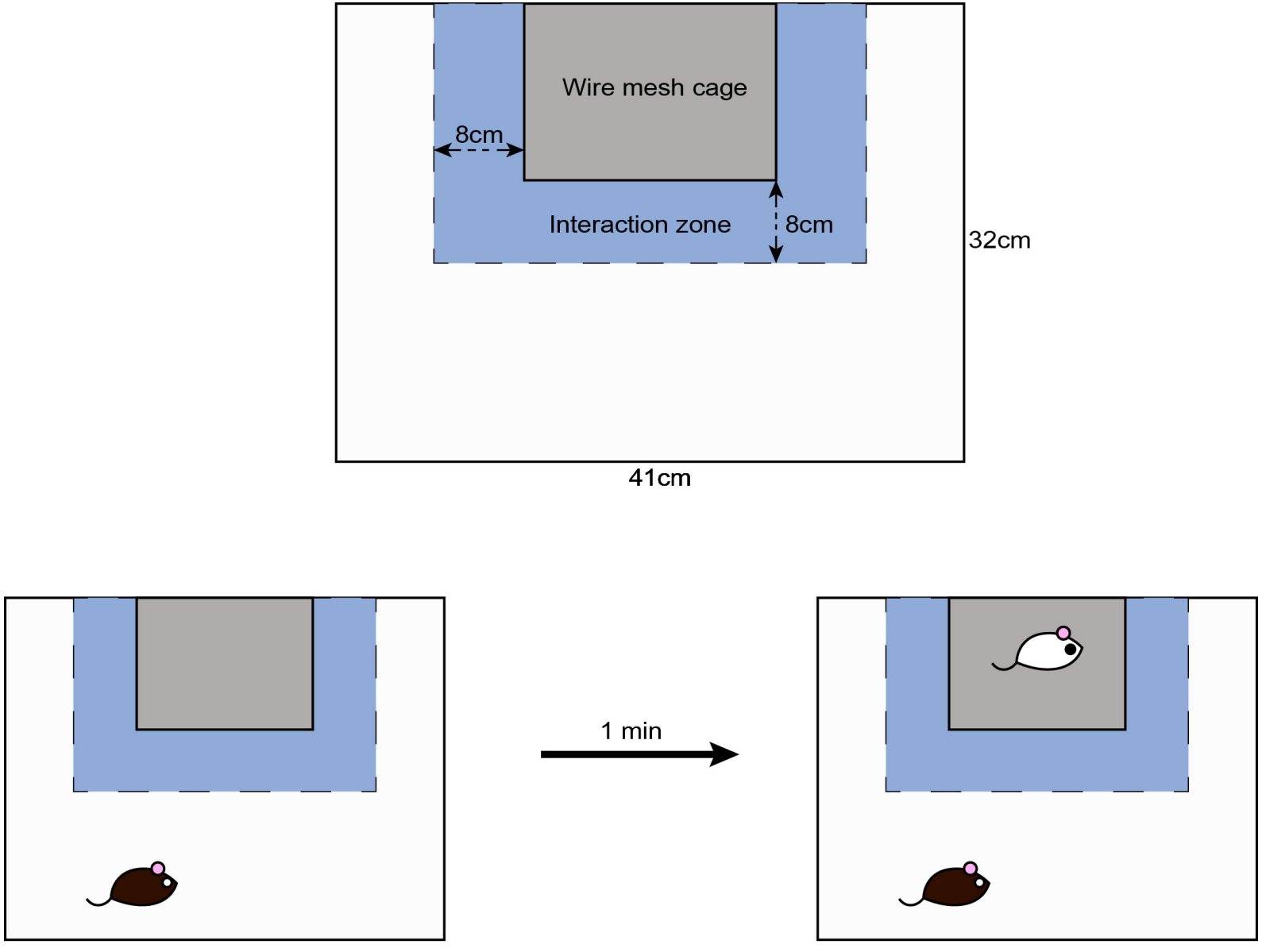
Wire mesh cage
8cm
Interaction zone
8cm
32cm
41cm
1 min
Trial 1 (2.5 min)
Trial 2 (2.5 min)

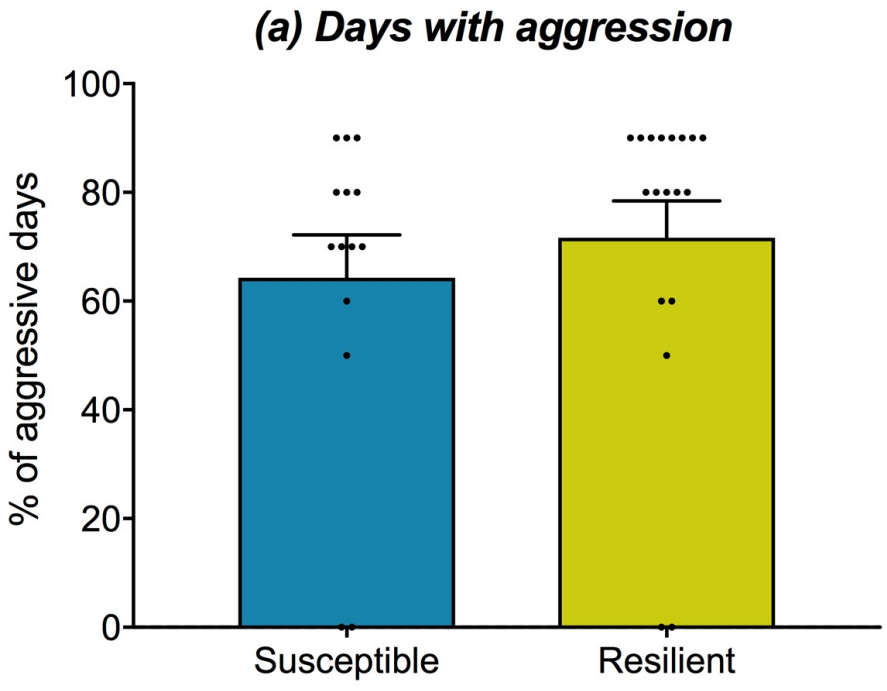
(a) Days with aggression
% of aggressive days
100
80
60
40
20
0
Susceptible
Resilient

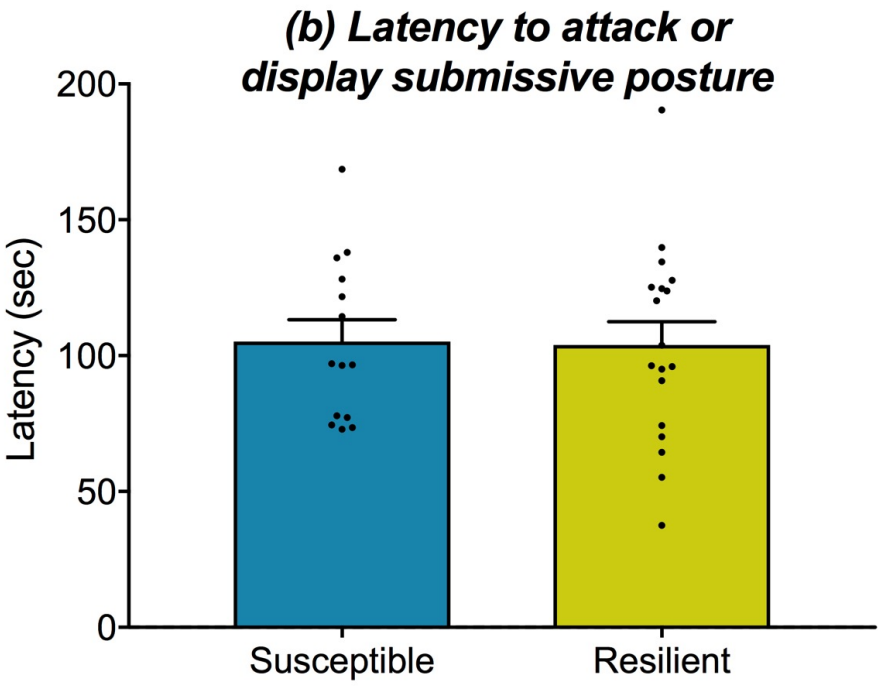
(b) Latency to attack or display submissive posture
Latency (sec)
200
150
100
50
0
Susceptible
Resilient